



HAL
open science

Spin-Valve Effect of the Spin Accumulation Resistance in a Double Ferromagnet - Superconductor Junction

Pengshun S. Luo, Thierry Crozes, Bruno Gilles, Sukumar Rajauria, Bernard Pannetier, Hervé Courtois

► **To cite this version:**

Pengshun S. Luo, Thierry Crozes, Bruno Gilles, Sukumar Rajauria, Bernard Pannetier, et al.. Spin-Valve Effect of the Spin Accumulation Resistance in a Double Ferromagnet - Superconductor Junction. 2008. hal-00341815v1

HAL Id: hal-00341815

<https://hal.science/hal-00341815v1>

Preprint submitted on 26 Nov 2008 (v1), last revised 3 May 2009 (v2)

HAL is a multi-disciplinary open access archive for the deposit and dissemination of scientific research documents, whether they are published or not. The documents may come from teaching and research institutions in France or abroad, or from public or private research centers.

L'archive ouverte pluridisciplinaire **HAL**, est destinée au dépôt et à la diffusion de documents scientifiques de niveau recherche, publiés ou non, émanant des établissements d'enseignement et de recherche français ou étrangers, des laboratoires publics ou privés.

Spin-Valve Effect of the Spin Accumulation Resistance in a Double Ferromagnet - Superconductor Junction

P. S. Luo,¹ T. Crozes,¹ B. Gilles,² S. Rajauria,¹ B. Pannetier,¹ and H. Courtois^{1,*}

¹*Institut Néel, C.N.R.S. and Université Joseph Fourier,
25 Avenue des Martyrs, 38042 Grenoble, France.*

²*SIMAP, C.N.R.S., Université Joseph Fourier and Grenoble I.N.P.,
Domaine Universitaire, 1130 rue de la Piscine, 38402 Saint Martin d'Hères, France*

(Dated: November 26, 2008)

We have measured the transport properties of Ferromagnet - Superconductor nanostructures, where two superconducting aluminum (Al) electrodes are connected through two ferromagnetic iron (Fe) ellipsoids in parallel. We find that, below the superconducting critical temperature of Al, the resistance depends on the relative alignment of the ferromagnets' magnetization. This spin-valve effect is analyzed in terms of spin accumulation in the superconducting electrode submitted to inverse proximity effect.

At a Normal metal-Superconductor (N-S) junction biased at a voltage below the superconducting gap Δ/e , Andreev reflection is the dominant contribution to transport. Here, one spin-up electron penetrates the superconductor with a spin-down electron so that a Cooper pair is formed. This can also be viewed as the reflection of an electron into a hole [1]. Since the two electron spin populations are involved, Andreev reflection is reduced in a F-S junction based on a Ferromagnetic (F) metal, and even suppressed in the case of a full spin-polarization [2]. Crossed Andreev Reflections (CAR) is predicted to occur in a geometry where two normal metal leads are in contact with one superconductor with an inter-distance at most of the order of the superconducting coherence length ξ_s [3]. Here, one electron coming from one lead and impinging the superconducting interface is reflected as a hole in the other lead. Similarly, an electron can travel through the superconductor from one lead to the other by elastic co-tunneling (EC) [4]. Experiments on multi-terminal F-S structures with two close ferromagnetic probes showed a non-local signal sensitive to the relative magnetization alignment [5]. This was attributed to CAR, which would be enhanced in an anti-parallel state (AP) and inhibited in a parallel (P) magnetization state. A similar bias-dependent non-local signal was observed in N-I-S-I-N planar junctions (I stands for Insulator) [6] and N-S multiterminal devices [7].

At the interface between a spin-polarized (usually ferromagnetic) conductor and a superconductor, a spin-polarized current is converted into a spinless current [8]. This conversion occurs in the ferromagnetic metal on a characteristic length scale given by the spin relaxation length λ_{sf} . It generates an accumulation of electrons with the minority spin close to the interface, which induces an extra resistance of amplitude determined by a length λ_{sf} of the ferromagnetic metal. Although non-local mechanisms and spin accumulation effects can co-exist in hybrid F-S nanostructures, their relative contribution to electron transport has been little studied.

In this letter, we address the spin-dependent transport in hybrid F-S nanostructures at the junction between two ferromagnetic leads and a superconductor. In the superconducting state, we observe a bias-dependent spin-valve effect, which we discuss in terms of different mechanisms, including non-local effects and spin accumulation. We conclude that the observed spin-valve effect is due to spin accumulation in the superconducting electrode submitted to a significant inverse proximity effect.

Fig. 1 a, b show the two sample geometries that we have investigated. In every case, two superconducting Al reservoirs or wires are connected through two Fe ellipsoids in parallel. We have chosen an ellipsoidal shape in order to obtain a single magnetic domain regime within one ellipsoid. The spacing between the Fe ellipsoids was varied between 100 and 500 nm. The separation between the two Al reservoirs is 100 nm. The latter is much larger than the proximity effect decay length in a ferromagnetic metal, which means that the two superconducting interfaces of an ellipsoid are decoupled. Geometry a) is designed to have voltage probes close to the F-S interface, while geometry b) reduces significantly the influence on the superconducting electrodes of the stray field induced at the ellipsoids ends. The fabrication procedure starts from epitaxial Fe films that were grown on a MgO substrate at room temperature under a residual pressure below 10^{-9} mbar and annealed at 600 °C for 3 h. The films are 40 nm thick and protected by a 3 nm layer of Pt or Au. First, the Fe ellipsoids are patterned by e-beam lithography and Ar ion-etching. After a second e-beam lithography, a 70 nm Al film is deposited on a resist mask and lifted-off. Prior to the deposition of Al, the protection layer is removed by a soft ion-milling.

In a given sample, the two ellipsoids have been made with different dimensions (900×100 nm² and 500×150 nm²) in order to obtain different coercive fields. Fig. 1c displays the topographical and the magnetic images of the same area of a test sample featuring a large number of Fe ellipsoids pairs. The magnetic images were acquired

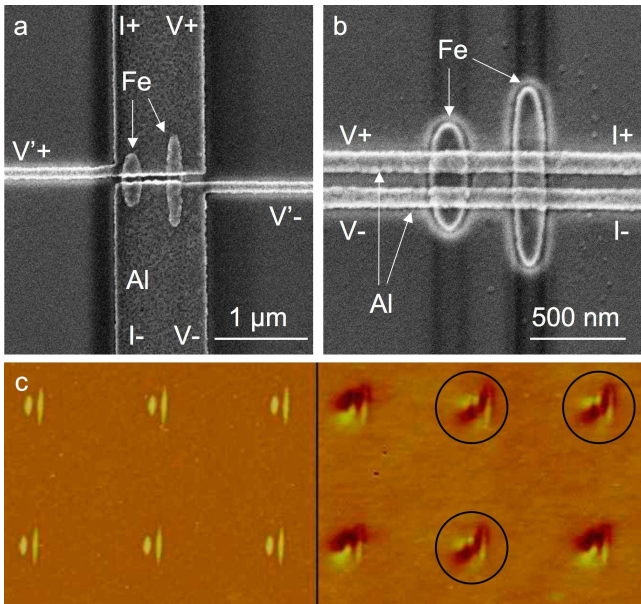


FIG. 1: Top: Micrographs of the two sample geometries based on a Fe ellipsoids pair together with the measurement connections. (a) The two wide Al pads have voltage probes close to the interface. (b) The two Al wires do not overlap the ends of the ellipsoids, where the largest stray field is induced. Bottom: (c) Topographical (left) and magnetic (right) images of the same area of a test sample made of a large number of Fe ellipsoids pairs. The magnetic image has been taken at a magnetic field of 30 mT after having polarized the sample in the opposite direction at - 200 mT. The pairs indicated by a circle show an anti-parallel (AP) magnetization state.

with a Magnetic Force Microscope (MFM) and give access to the perpendicular to the surface component of the magnetic field gradient. Fig. 1c data was acquired at a moderate in-plane magnetic field of 30 mT after full polarization of the sample in the opposite direction at - 200 mT. For every ellipsoid, the magnetic image is compatible with a single magnetic domain configuration. Although all ellipsoids pairs were made identically, part of them show an AP magnetization configuration, meaning that the short ellipsoid has switched while the long one remains pinned. This scattering is presumably due to slight changes in the precise ellipsoids geometry. For instance, it is expected that the ellipsoid edge roughness plays a significant role in the exact value of the coercive field. Based on the full series of measurements, we find that the switching fields of the ellipsoids are about 30 mT for the short one and 50 mT for the long one, with significant variations from one sample to the other.

We have measured the electron transport properties of a series of samples at very low temperature down to 260 mK. We used a lock-in technique with an a.c. current with an amplitude of 100 to 200 nA superposed to a d.c. bias current. Here we present experimental data from one sample (Sample 5) out of 8 samples, all showing a

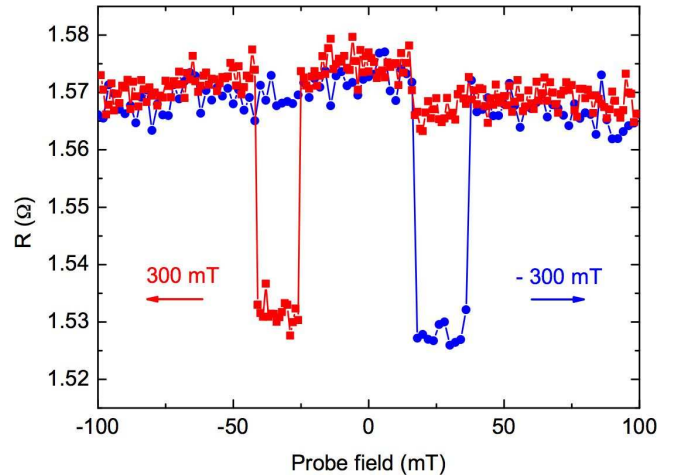


FIG. 2: (Color online) Probe magnetic field dependence of Sample 5 zero-bias differential resistance at 310 mK. Red square (blue circular) dots: the Fe ellipsoids are first polarized with + (-) 300 mT magnetic field and the differential resistance is measured at zero external magnetic field with decreasing (increasing) probe fields.

similar behavior. It is of geometry a) and was measured in a 2-wire configuration, unless otherwise specified. The measurements presented here have been done at zero applied magnetic field.

Let us first discuss the spin-valve effects in our samples. At the beginning of a measurement, we polarize the two ellipsoids magnetizations with a magnetic field of absolute value 300 mT. Afterwards and for every data point, we apply for about 1 s a probe magnetic field of a varying value. The field is then ramped back to zero and the resistance is measured. This procedure is repeated at a series of values for the probe magnetic field starting from the polarization field and until a field opposite in sign is reached. In this way, we can systematically measure the resistance of the device in different magnetization configurations, without the parasitic effects of a non-zero magnetic field.

Fig. 2 shows an example of such a measurement, where the horizontal axis indicates the probe magnetic field that was applied just before the measurement. We observe sharp stepwise changes of the resistance, with two symmetric domains featuring a lower value. The values of the probe magnetic field at the resistance changes are compatible with the switching fields of the two different ellipsoids. In this respect, we ascribe the low-resistance domains to the regime of AP magnetizations ($\uparrow\downarrow$ or $\downarrow\uparrow$). Both at smaller field and at higher field, the resistance is higher and constant within the measurement accuracy. We ascribe these states to a P configuration ($\downarrow\downarrow$ or $\uparrow\uparrow$). The resistance difference between the AP and the P states is about 40 mΩ or 3 %. This spin-valve effect is the central result of this paper.

Let us now describe our further experimental study

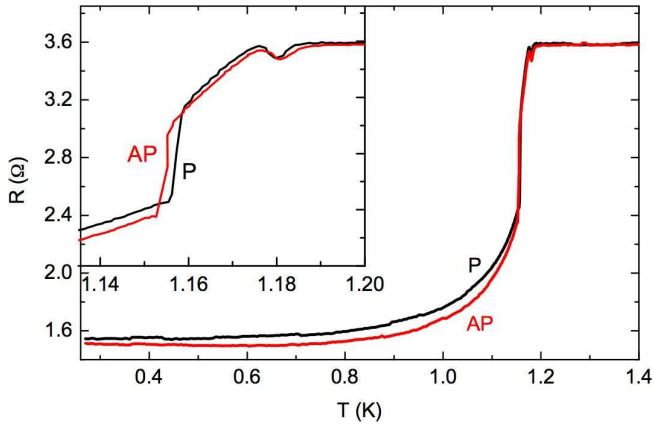


FIG. 3: Temperature dependence of Sample 5 zero-bias resistance in parallel (P) and anti-parallel (AP) magnetization states. The inset shows a zoom close the Al superconducting critical temperature.

and data analysis aimed at identifying the involved physical effect. Based on the previous measurement technique, we can prepare the sample in a P or AP state and sweep either the current bias or the temperature. Fig. 3 displays the temperature dependence of Sample 5 resistance in both P and AP states. We observe that the spin-valve effect amplitude has a non-monotonous behavior, with a maximum at about 0.9 K. At lower temperature, it decreases steadily towards zero. Most importantly, the effect is absent within a $1\text{ m}\Omega$ resolution above the critical temperature $T_c = 1.18\text{ K}$ of Al. The observed spin-valve effect is thus related to superconductivity. Fig. 3 inset shows that the magnetic state has also a small effect (about 3 mK) on the critical temperature of the Al electrodes. This can be due to the dipolar magnetic field arising from the ellipsoids magnetization, or to a spin-sensitive proximity effect [9]. At low temperature, the same mechanism may also modify the superconducting gap and hence influence the transport properties. Nevertheless, as geometry a) and b) samples show a similar behavior although geometry b) is much less sensitive to stray field, we conclude that the stray field effect does not explain the observed spin-valve effects.

Fig. 4 left shows Sample 5 differential resistance in different magnetic states. In the data presented here, the voltage across the junction remains well in the sub-gap regime. In the AP states, we find a zero-bias resistance peak, which is suppressed in the P states. The spin valve effect is larger for finite voltage bias, which is consistent with the above observation that it is larger at finite temperature. The two P states on one side and the two AP states on the other side behave very similarly. This confirms that the electron transport in our samples depends primarily on the relative magnetization alignment of the two ellipsoids, not on the direction of a given magnetization.

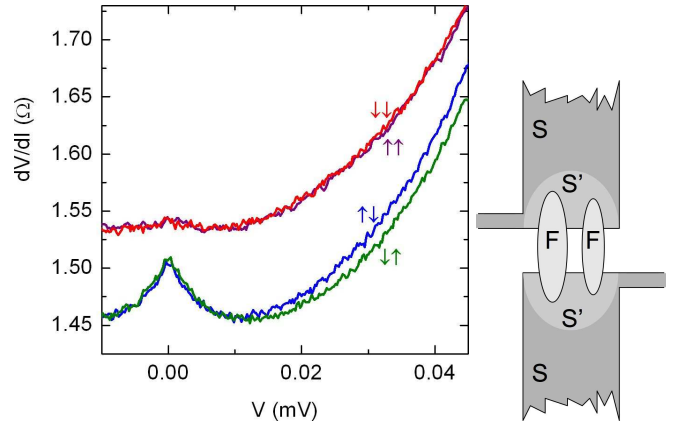


FIG. 4: Left: Sample 5 differential resistance dV/dI as a function of voltage V in the two parallel (P) (top curves, $\downarrow\downarrow$ and $\uparrow\uparrow$) and the two anti-parallel (AP) states (bottom curves, $\uparrow\downarrow$ and $\downarrow\uparrow$). Right: Schematics of the sample geometry a) outlining the region S' of the superconducting electrodes S submitted to inverse proximity effect and where spin accumulation is expected to occur.

Table 1 lists the main properties of the 8 investigated samples, showing a spin-valve effect as discussed above. The spin-valve effect amplitude ΔR varies quite little, between 18 to $43\text{ m}\Omega$. It does not show a correlation with the sample resistance or with the ellipsoids separation. In the geometry a), we have probed the resistance either in a 2 wires geometry by using the wide Al electrodes for both current bias and voltage measurement, or in a 4 wires geometry by using voltage probes in the vicinity of the F-S interfaces. We observed an identical low temperature behavior in both cases. In a 4-wire configuration, a resistance peak appears close to the critical temperature, due to the charge-imbalance in the superconductor [10].

Let us now turn to the interpretation of the observed spin-valve effects. As for non-local effects, EC from one ferromagnetic ellipsoid to the other would have no contribution here, since we measure the total current flowing through the two ellipsoids in parallel. The sign and amplitude of the measured effect are compatible with CAR, but the absence of significant influence of the ellipsoids separation in the 100-500 nm range, whereas the superconducting coherence length ξ_s is estimated to be about 100 nm, discards an interpretation in terms of CAR.

A significant inverse proximity effect is expected in a superconductor S in the vicinity of a transparent contact with a ferromagnetic metal F , see Fig. 4 right part. The sub-gap electronic density of states is non-zero in a region S' of the superconductor extending over a few times the superconducting coherence length [11]. This allows for the injection at a sub-gap bias of spin-polarized quasi-particles from the two Fe ellipsoids into every Al electrode. In a P state, the current through both ellipsoids injects the same majority of spins and a significant spin accumulation builds up in the S' region of the Al

Sample	Geometry	Separation (nm)	$R_n(\Omega)$	$\Delta R(\Omega)$
1	a	150	11.0	0.022
2	a	150	7.048	0.041
3	a	150	6.178	0.023
4	b	100	1.191	0.018
5	a	150	3.585	0.043
6	b	150	6.60	0.024
7	b	150	18.0	0.018
8	b	500	4.01	0.023

TABLE I: Sample parameters including the geometry type, the separation between the two Al ellipsoids, the normal-state resistance R_n and the spin-valve effect amplitude ΔR at 300 mK.

electrode. In a AP state, one ellipsoid injects spin-up quasi-particles and the other one injects spin-down quasi-particles. The two spin populations are then balanced and little spin accumulation is expected. Thus we expect that, due to spin accumulation, a AP state has a lower resistance than a P state, as observed in the experiment. The considered spin-accumulation resistance builds up in the superconductor. No such effect is expected in the absence of inverse proximity effect, in which case spin accumulation occurs separately in the two leads.

In the case of a plain F-S interface, the magnitude of the spin accumulation induced resistance is [8]: $\Delta R = R_{sq} \cdot (\lambda_{sf}/w) \cdot (\alpha^2/(1 - \alpha^2))$, where R_{sq} is the square resistance, w the wire width and α is the spin polarization. Taking into account a square resistance R_{sq} of 1Ω , a wire width w of 400 nm, a spin relaxation length λ_{sf} of 400 nm in Al [12] and a polarization α of 40 % close to the one of bulk Fe [13], one obtains $\Delta R = 0.02 \Omega$ per interface, in fair agreement with the resistance change amplitude at zero bias. The spin polarization in the Al electrode is presumably smaller than in bulk Fe, which would decrease the amplitude of the effect. In contrast, superconductivity can enhance the spin-accumulation resistance [14, 15] and therefore the amplitude of the related spin-valve effect. Eventually, the dependence on bias and temperature of the spin-valve effect can be related to changes of the size of the region under inverse proximity effect S'. As the current bias or the temperature increases, the inverse proximity effect extends over a larger distance and the spin accumulation effects increase.

In conclusion, we have investigated the sub-gap transport properties in double F-S hybrid structures with two F elements. Below the critical temperature of the superconductor, the resistance depends on the relative magnetization alignment. This spin-valve behavior is related to the spin accumulation in the superconducting electrode

submitted to a significant inverse proximity effect. This approach is similar to considering a out-of-equilibrium region in the vicinity of the interface [16] and it may also hold for previous experiments in similar hybrid nanostructures [17].

The samples have been fabricated at Nanofab-C.N.R.S. Grenoble plat-form. We acknowledge support from "Elec-EPR" ANR contract and STREP "SFInx" EU project. We acknowledge the contribution of M. Giroud at the early stage of this project. We thank I. L. Prejbeanu for MFM characterizations measurements, D. Beckmann and R. Mélin for discussions.

* herve.courtois@grenoble.cnrs.fr; Also at Institut Universitaire de France

- [1] A. F. Andreev, *Zh. Eksp. Teor. Fiz.* **46**, 1823 (1963) [*Sov. Phys. JETP* **19**, 1228 (1964)]; D. Saint-James, *J. Phys. (Paris)* **25**, 899 (1964).
- [2] M. J. M. de Jong and C. W. J. Beenakker, *Phys. Rev. Lett.* **74**, 1657 (1995).
- [3] J. M. Byers and M. E. Flatté, *Phys. Rev. Lett.* **74**, 306 (1995); G. Deutscher and D. Feinberg, *Appl. Phys. Lett.* **76**, 487 (2000).
- [4] G. Falci, D. Feinberg and F. W. J. Hekking, *Europhys. Lett.* **54**, 255 (2001); R. Mélin and D. Feinberg, *Eur. Phys. J. B* **26**, 101 (2002); J. P. Morten, A. Brataas, and W. Belzig, *Phys. Rev. B* **74**, 214510 (2006).
- [5] D. Beckmann, H. B. Weber, and H. v. Löhneysen, *Phys. Rev. Lett.* **93**, 197003 (2004).
- [6] S. Russo, M. Kroug, T. M. Klapwijk, and A. F. Morpurgo, *Phys. Rev. Lett.* **95**, 027002 (2005); A. L. Yeyati, F. S. Bergeret, A. Martin-Rodero, T. M. Klapwijk, *Nature Phys.* **3**, 455 (2007).
- [7] P. Cadden-Zimansky and V. Chandrasekhar, *Phys. Rev. Lett.* **97**, 237003 (2006).
- [8] F. J. Jedema, B. J. van Wees, B. H. Hoving, A. T. Filip and T. M. Klapwijk, *Phys. Rev. B* **60**, 16549 (1999).
- [9] A. Yu. Rusanov, M. Hesselberth, J. Aarts, and A. I. Buzdin, *Phys. Rev. Lett.* **93**, 057002 (2004).
- [10] J. Clarke, *Phys. Rev. Lett.* **28**, 1363 (1972); A. Schmid and P. Martinoli, *J. of Low Temp. Phys.* **20**, 207 (1975).
- [11] M. A. Sillanpää, T. T. Heikkilä, R. K. Lindell, and P. J. Hakonen, *Europhys. Lett.* **56**, 590 (2001).
- [12] M. V. Costache, M. Zaffalon, and B. J. van Wees, *Phys. Rev. B* **74**, 012412 (2006).
- [13] I. I. Mazin, *Phys. Rev. Lett.* **83**, 1427 (1999).
- [14] N. Poli, J. P. Morten, M. Urech, A. Brataas, D. B. Haviland, and V. Korenivski, *Phys. Rev. Lett.* **100**, 136601 (2008).
- [15] S. Takahashi and S. Maekawa, *Phys. Rev. B* **67**, 052409 (2003).
- [16] R. Mélin, *Phys. Rev. B* **72**, 054503 (2005).
- [17] M. Giroud, K. Hasselbach, H. Courtois, D. Maily, and B. Pannetier, *Eur. Phys. J. B* **31**, 103 (2003).